Molecular Autism

RESEARCH

Open Access

White matter microstructure as a potential contributor to differences in resting state alpha activity between neurotypical and autistic children: a longitudinal multimodal imaging study

Guannan Shen[1,8*], Heather L. Green[1], Marybeth McNamee[1], Rose E. Franzen[1], Marissa DiPiero[1], Jeffrey I. Berman[1,2], Matthew Ku[1], Luke Bloy[1], Song Liu[1], Megan Airey[1], Sophia Goldin[1], Lisa Blaskey[1,2,3], Emily S. Kuschner[1,3,4], Mina Kim[1], Kimberly Konka[1], Gregory A. Miller[5,6,7] and J. Christopher Edgar[1,2]

Abstract

We and others have demonstrated the resting-state (RS) peak alpha frequency (PAF) as a potential clinical marker for young children with autism spectrum disorder (ASD), with previous studies observing a higher PAF in school-age children with ASD versus typically developing (TD) children, as well as an association between the RS PAF and measures of processing speed in TD but not ASD. The brain mechanisms associated with these findings are unknown. A few studies have found that in children more mature optic radiation white matter is associated with a higher PAF. Other studies have reported white matter and neural activity associations in TD but not ASD. The present study hypothesized that group differences in the RS PAF are due, in part, to group differences in optic radiation white matter and PAF associations. The maturation of the RS PAF (measured using magnetoencephalography(MEG)), optic radiation white matter (measured using diffusion tensor imaging(DTI)), and associations with processing speed were assessed in a longitudinal cohort of TD and ASD children. Time 1 MEG and DTI measures were obtained at 6–8 years old (59TD and 56ASD) with follow-up brain measures collected ~ 1.5 and ~ 3 years later. The parietal-occipital PAF increased with age in both groups by 0.13 Hz/year, with a main effect of group showing the expected higher PAF in ASD than TD (an average of 0.26 Hz across the 3 time points). Across age, the RS PAF predicted processing speed in TD but not ASD. Finally, more mature optic radiation white matter measures (FA, RD, MD, AD) were associated with a higher PAF in both groups. Present findings provide additional evidence supporting the use of the RS PAF as a brain marker in children with ASD 6–10 years old, and replicate findings of an association between the RS PAF and processing speed in TD but not ASD. The hypothesis that the RS PAF group differences (with ASD leading TD by about 2 years) would be explained by group differences in optic radiation white matter was not supported, with brain structure-function associations indicating that more mature optic radiation white matter is associated with a higher RS PAF in both groups.

Keywords Autism spectrum disorder, Magnetoencephalography, Peak alpha frequency, Maturation, DTI

*Correspondence:
Guannan Shen
sheng1@chop.edu
Full list of author information is available at the end of the article

Introduction

In the eyes-closed resting-state (RS), alpha oscillations (7 to 13 Hz in adults) are the dominant rhythm, most prominent in parieto-occipital regions [30, 39, 71]. Notable in children is an age-related increase in the frequency at which RS alpha oscillations show maximum power, often referred to as the peak alpha frequency (PAF). Among electroencephalography (EEG) and magnetoencephalographic (MEG) measures, the RS PAF is a robust signature of brain maturation [78, 83]. Studies show an alpha peak at ~7 Hz in young children (6 to 8 years old), with an adult profile not observed until late childhood or early adolescence [20, 60, 76]. The PAF shows promise as a clinical marker, showing high test and retest reliability [51] and is considered one of the most heritable brain measures [84, 85].

Among neurodevelopmental conditions, EEG and MEG studies have examined RS alpha activity in children with autism spectrum disorder (ASD)[1]. Several studies have reported a higher PAF in children with ASD than children with typical development (TD) [23, 28, 30, 73], but some studies have found no PAF group differences [12, 33, 50]. As detailed in Shen et al. [73], such differences are likely due to differences in the age of the study cohorts. In particular, given an age-related increase in the PAF in TD children [13, 57, 60, 76] but not in children with ASD [22, 28, 30, 32, 33, 50], we have proposed the RS PAF as an age-specific ASD brain marker [26, 28]. As an example, examining male children 6 to 18 years old, Edgar et al. [28] found that whereas in the younger children (6 to 10 years) the PAF was higher in ASD than TD, because the PAF values increased as a function of age in TD but not ASD. In the older children (10 to 18 years) the TD and ASD PAF values were similar, with the TD RS PAF having "caught up" to the ASD PAF. The higher PAF value in young children with ASD suggests more rapid brain maturation in ASD versus TD, mirroring a similar pattern of findings in structural brain development using magnetic resonance imaging (MRI) and diffusion tensor imaging (DTI) [6, 8, 16].

A potential mechanistic contributor to such group effects is brain structure, but few studies have sought to identify the structural brain correlates of the RS PAF. The age-related increase in the RS PAF is thought to reflect, in part, an enhancement of processing efficiency due to the maturation of white-matter pathways [68]. In particular, it is hypothesized that the maturation of white-matter connections between the thalamus and the parietal-occipital RS alpha generators [35, 52, 80] plays an important role in maturation of RS alpha activity [30, 43, 44, 54] as well as in maturation of alpha power [42, 59, 77, 81]. DTI provides an estimate of the structural properties of white-matter fibers, such as fiber distribution, density, and myelination [49, 79], with DTI parameters quantifying tissue microstructure in measures of fractional anisotropy (FA), mean diffusivity (MD), radial diffusivity (RD) and axial diffusivity (AD). In TD adults, FA of white-matter pathways has been associated with the RS PAF [82]. A recent DTI and EEG study showed that more mature optic radiation white matter (i.e., increased FA) was associated with a more mature PAF (i.e., higher frequency) in TD children, adolescents, and adults 5 to 21 years old [11]. The present study evaluated the potential contribution of white-matter microstructure to the TD and ASD differences in the RS PAF via assessing (1) the maturation of the optic radiation, which is the white-matter tract connecting the thalamus and visual cortex, and (2) group differences in associations between optic radiation white matter and the RS PAF. Altered microstructure and neural function associations in ASD have been reported in studies examining auditory cortex neural activity and auditory radiation diffusion measures, with the latency of auditory M50 responses associated with auditory radiation FA in TD but not ASD children [10, 66, 67]. Based on findings from these three previous studies, a loss of an optic radiation and RS PAF association in children with ASD was hypothesized.

Finally, given the association between the PAF and general cognitive ability, with the PAF predicting individual differences in cognitive performance, such as verbal abilities [7], memory performance [48, 65], speed of processing [28, 46, 73], visual target detection [11, 21, 58, 72, 86], and general intelligence [36], the PAF is developmentally and clinically relevant, with two previous studies showing an association between the RS PAF and processing speed in TD but not ASD children [28, 73]. The present longitudinal multimodal study provided a better assessment of this association, with study findings (e.g., group differences in optic radiation white matter) identifying treatment targets that might modify RS alpha activity as well as cognitive ability.

A three-time-point longitudinal design provided the ability to assess the maturation of the RS PAF and optic radiation white-matter in children with and without ASD. Replicating previous findings, a higher PAF in ASD than TD in this young cohort was hypothesized. Associations between the PAF and processing speed in TD but not ASD were also hypothesized. Finally, associations between optic radiation DTI metrics and the PAF were also predicted, with DTI and PAF associations hypothesized to be stronger in TD than ASD.

[1] Individuals on the autism spectrum, their parents, and professionals in the field differ regarding the use of person-first (e.g., children with ASD) or identity first (e.g., autistic child) language (Kenny et al., 2016). With respect for divided opinions, both approaches to terminology are used here.

Methods

Participants

This study was approved by the Institutional Review Board of Children's Hospital of Philadelphia (CHOP). Parents gave written informed consent, and the children verbal and written assent. Study data were obtained from a longitudinal multimodal neuroimaging study (R01 MH107506). TD children and autistic children 6 to 9 years old were recruited at Time 1. Although the study was designed so that the Time 1, 2 and 3 visits would occur ~ 18 months apart, a pause in data collection occurred due to COVID-19, resulting in some of the Time 2 and 3 visits occurring outside the 18-month interval (details follow). TD and ASD chidlren were selected according to the following criteria: (a) native English speakers, (b) no history of traumatic brain injury or other neurlogical condition such as history of seizures, (c) no genetic syndromes with an extremely high incidence of ASD (e.g., Fragile X), (d) no intellectual disability, (e) no premature birth, (f) no uncorrectable sensory impairments, (g) no contraindications for MRI such as metal implants, and (h) no neuroleptic/antipsychotic medication, guanfacine (for attention-deficit/hyperactivity disorder or ADHD), or SSRI treatment at Time 1. Participants taking stimulant medications were required to withhold medication for 24–36 h prior to their visit.

At Time 1, ASD participants had a prior diagnosis, made according to the Diagnostic Statistical Manual - Fifth Edition (DSM-5; [3]) criteria by a clinician at CHOP or by autism specialists in the community. A targeted diagnostic battery administered at Time 1 confirmed the original diagnosis in the ASD group and ruled out ASD in the TD group. ASD diagnosis was confirmed by the Autism Diagnostic Observation Schedule - Second Edition (ADOS-2; [55]) and parent report on the Social Communication Questionnaire (SCQ; [69]). Dimensional symptom severity indices were obtained by parent report on the Social Responsiveness Scale - Second Edition (SRS-2; [14]).

Members of the TD group were evaluated by licensed study psychologists who ruled out the presence of DSM-5 diagnoses based on clinical judgment, review of the child's medical history form, parent interview, parent ratings on standardized behavior questionnaires (i.e., Child Behavior Checklist (CBCL; [1])), Behavior Rating Inventory of Executive Functioning - Second Edition (BRIEF-2; [34]), and cognitive testing completed by the child at each of their visits. TD-specific inclusion criteria included scoring below the cut-off for autism concern on the SCQ and SRS-2 parent questionnaires. Additional TD-inclusion criteria included no first-degree relatives with ASD and no history of speech/language disorder, learning disability, ADHD, or psychiatric disorders. To rule out intellectual disability in both groups, an estimated nonverbal intelligence quotient (NVIQ) ≥ 70 on the Wechsler Intelligence Scale for Children - Fifth Edition (WISC-V; [88]), was required. WISC-V Symbol Search subtest score served as a measure of processing speed.

Group demographics for the children with evaluable MEG data are listed in Table 1. MEG data were obtained from 64 TD and 68 ASD children at Time 1. Reasons for unevaluable RS data included excessive motion, significant artfact due to movement, or the child unable to keep their eyes closed or complete the exam. The number of children with evaluable MEG and DTI data is also provided in Table 1 (final column). Time 2 data were obtained, on average, 19 months after the Time 1 visit. Time 3 data were obtained, on average, 21 months after the Time 2 visit. Reasons for attrition following Time 1 were as follows: lab closure due to COVID-19 (Time 2: TD = 12, ASD = 11, Time 3: TD = 22, ASD = 18), and new exclusion diagnoses after Time 1 including diagnosis of depression ($N=2$), anxiety ($N=3$), attention deficit disorder ($N=2$), intermittent explosive disorder ($N=1$), or learning disability ($N=2$) in the TD children, and seizure disorder in the children with ASD ($N=3$).

Four ASD children with evaluable MEG data did not complete cognitive testing (Time 1 = 1, Time 2 = 1, Time 3 = 2). Seven ASD children (Time 1 = 3, Time 2 = 3, Time 3 = 1) and 3 TD children (all Time 1) did not complete the processing speed task. No Group differences were observed in Sex ($p=0.61$), Age ($p=0.1$), or NVIQ

Table 1 Participants with evaluable MEG RS data at each visit

	Group	*N*	Sex (Female)	Age years (SD)	NVIQ: Fluid Reasoning (SD)	SRS: T-score (SD)	Processing speed: Symbol Search (SD)	*N*: MEG + DTI
Time 1	TD	59	12	7.4 (0.8)	110 (14)	45 (7)	10 (3)	55
	ASD	56	9	7.8 (0.8)	104 (16)	72 (12)	9 (3)	45
Time 2	TD	41	7	9.0 (0.8)	109 (14)	44 (7)	10 (3)	38
	ASD	49	8	9.2 (0.9)	107 (16)	68 (11)	9 (4)	37
Time 3	TD	37	6	10.8 (0.8)	110 (13)	45 (10)	10 (3)	34
	ASD	39	5	10.9 (0.9)	107 (17)	69 (8)	8 (4)	28

($p=0.15$) across Time ($ps>0.05$). The TD cohort had a higher Processing Speed score than the ASD cohort across Time ($p=0.003$). In the ASD cohort, there were no differences in Time 1 SRS-2 scores between the children who returned for the Time 3 visit ($N=30$) and the children who did not return for the Time 3 visit ($N=26$; $p=0.60$).

MEG data acquisition and MRI data acquisition and data processing

Eyes-closed RS MEG data were obtained from TD and ASD children using a 275-channel MEG system (VSM MedTech Inc., Coquitlam, BC). Children were instructed to close their eyes for 5–7 min. During the course of the study the length of the RS exam was increased to ensure sufficient data for future functional connectivity analyses. Electro-oculogram ((EOG), vertical EOG above and below the left eyes) and electrocardiogram (ECG) were obtained. The EOG channel was monitored during recording, and if the child opened their eyes during the exam they were reminded to close them. After applying a band-pass filter (0.03–150 Hz), EOG, ECG, and MEG signals were digitized at 600 Hz with 3rd-order gradiometer environmental noise reduction. Head position was monitored using four head position indicator (HPI) coils attached to the scalp. Children were scanned in a supine position.

After the MEG session, structural and diffusion MRI (dMRI) data were obtained using a Siemens Prisma 3T MR system with a 32-channel head coil. All MRI data were acquired while participants watched a movie of their choice. T1-weighted magnetization-prepared rapid gradient-echo (MP-RAGE) structural images were collected with $0.8\times0.8\times0.8$ mm^3 spatial resolution. dMRI data were obtained using the HCP Lifespan diffusion protocol [40]. The diffusion acquisition included four 5.5-minute sequences. Diffusion sequence parameters were TR = 3222 ms, TE = 89.2 ms, and a 1.5 mm isotropic resolution. A total of 14 b = 0 volumes, 93 b = 1500 s/mm^2, and 92 b = 3000 s/mm^2 volumes were aquired with both anterior-to-posterior (AP) and posterior-to-anterior (PA) phase encoding. The 4 sequences were aquired with phase encoding directions ordered AP, PA, AP, PA for eddy-current correction. Thus, in total 398 volumes were acquired.

DTI data processing

Distortion correction based on the phase encoding pairs was performed with topup [4]. To correct for artifacts from eddy currents, head movements, and intravolume movement, eddy_cuda was run on a graphics processing unit (GPU) cluster [5]. Images were visually inspected for motion artifacts and manually corrected if automatic processing failed.

DTI parameter maps including fractional anisotropy (FA), mean difusivity (MD), radial diffusivity (RD), and axial diffusivity (AD) were computed using the dtifit function of the FMRIB Diffusion Toolbox (FMRIB Software Library; [74, 90]. Registration of each subject's FA map to the Montreal Neurological Institute (MNI) template was performed using FMRIB FNIRT to obtain DTI parameters from a visual cortex region of interest (ROI), capturing the distal portion of the optic radiations. Optic radiation diffusion measures were obtained via averaging across voxels in the left and right optic radiation ROI. No group differences were observed for the DTI motion estimates ($p=0.21$).

MEG data processing

MEG data were processed using BESA Research 7.1, co-registering each child's MEG data to their T1-weighted MRI data using BESA MRI 3.0 (MEGIS Software GmbH, Grafelfing, Germany). To represent the 275-channel MEG data in a smaller number of measures for analysis, a source model with 15 regional sources was applied to project each child's raw MEG surface data into brain source space [15, 28, 73]. A two-step process was employed for removal of muscle and movement artifact, with the following steps done blind to diagnosis. First, the child's EOG and scalp MEG data were visually examined to remove epochs with blinks, saccades, or other significant EOG activity from the MEG data. Second, each child's MEG data were visually inspected for muscle-related activity, with a focus on data from sensors close to the temporalis muscles, and epochs containing muscle activity were removed. After artifact removal, across Group and Time the average child had 3 + minutes of evaluable RS data: 264 s for ASD (SD = 90 s, range = 28 to 377 s) and 277 s for TD (SD = 75 s, range = 73 to 379 s). A linear mixed effects model was conducted on the amount of non-artifact RS data with factors Age and Group. A main effect of Age and Group indicated an increase of usable data by 35 s per year ($p<0.001$), and more evaluable data for TD than ASD ($p=0.01$). As detailed in the Online Supplement, Group differences in the amount of non-artifact RS data were relatively small (Supplement Table 1), and the amount of artifact-free RS data did not affect the detection of the PAF (Supplement Fig. 1). In additon, posthoc analyses examining PAF values obtained by segmenting a child's recording ($N=10$ TD and 10 ASD) into datasets of 7 durations (30 s, 60 s, 90 s, 120 s, 150 s, 180 s, 210 s) showed high reliability of the PAF value across the 7 durations (PAF ICC = 0.96).

MEG data were transformed from scalp space to brain source space and then from the time domain to

the frequency domain, applying a Fast Fourier Transform to artifact-free 3.41 s epochs of continuous data for each of the two orthogonally oriented time series at each regional source. Each 3.41 s epoch overlapped 50% with the next epoch, and each epoch was multiplied by a cosine squared window, resulting in power spectra with a frequency resolution of 0.29 Hz. This combination of overlap and windowing ensured that each time point contributed equally to the mean power spectra. When the segment of data following an artifact-free epoch was bad, there was no overlap between epochs, and windowing was thus applied to the next available artifact-free 3.41 s epoch. The mean power spectra across the epochs for the two orthogonally oriented time series at each regional source were summed to yield the power at a given frequency at the source.

To obtain a measure of the RS PAF, the specparameterization method and toolbox of Donoghue et al. [25], an open-source Python Package (https://specparam-tools.github.io) in Python (version 3.7), was used to separate the aperiodic (1/f) component of the RS power spectrum from RS periodic oscillatory activity. Ostlund et al. [63] provide a detailed review of this method. Spectral parameterization was performed on the power spectra at all 15 sources using the following settings: peak_width_limits = [1, 8], min_peakheight = 0.1, max_number_of_peaks = 6, frequency_range = [3, 40] Hz, overlap threshold = 2 SD. As described in Ostlund et al. [63], the following steps were applied to obtain estimates of the RS oscillatory peaks and the aperiodic offset and exponent measures. First, an initial aperiodic fit was applied to the power spectrum and removed, with the residual activity fitted with a Gaussian function (using the above specparam settings). After the fitted oscillatory peaks were removed, the aperiodic activity was re-fit. Finally, the fitted aperiodic and periodic oscillatory signals were combined and goodness-of-fit assessed (described with R^2 and Mean Absolute Error (MAE)). After the initial parameterazation fit, a knee (in specparam terminology) was observed in the aperiodic component in a majority of the subjects (across Age and Group). Therefore, a knee parameter was included in the specparam parameterization. (As a comparison, the Pearson's correlation between the PAF values estimated with and without knee was $r = 0.86$, $p < 0.05$,) The present study reports model fit (R^2 and MAE) and the specparam alpha central frequency value (mean of the Gaussian).

At each visit, a single PAF value per child was identified via examining activity at the 9 posterior sources, as RS alpha activity is most prominent in parietal-occipital regions [28, 30, 39, 61]. In particular, the PAF was obtained examining RS power spectra at central (left, midline, right), parietal (left, midline, right), and ventral (posterior temporal left, occipito-polar midline, posterior temporal right) sources. A single PAF value for each child was obtained via: (1) identifying the central frequency of the oscillatory peak with the most power between between 7 and 13 Hz at each source, and (2) identifying a single frequency with the most alpha power (i.e., the PAF) across the 9 sources. Across the Groups, the PAF was identified in the 9 posterior locations as follows: occipito-polar midline (46%), parietal midline (39%), parietal right (4%), central right (4%), posterior temporal left (2%), central left (2%) and central midline (2%). A chi-square test showed that TD and ASD did not differ in the location where the PAF was identified ($p = 0.40$).

Statistical analysis

Statistical analyses were performed using R (version 4.2.2). Linear mixed effects models (LMM), executed with the lme4 package [9], examined the association of PAF with Age, Group, and Age x Group. Age was centered by subtracting 6.1 years (the youngest age of the cohort). Random intercept terms were included to account for within-subject correlations between visits. Inclusion of the random slope was evaluated based on the smallest Akaike Information Criterion (AIC) value. Similar LMMs were conducted for all four diffusion measures (RD, AD, MD and FA), evaluating the maturation of the optic radiation as well as optic radiation Group differences. Associations between the DTI measures and the PAF were assessed using LMMs, with the PAF as the outcome measure. Effects of DTI, Age, Group, and Group x DTI interaction were considered. Finally, associations between the PAF and estimates of ASD symptom severity (SRS-2 score) and processing speed (WISC-V Symbol Search score) were examined using LMMs with cognitive or behavioral score as the outcome variable. Effects of PAF, Group, and Group x PAF were evaluated based on AIC values.

Results

Specparam model goodness-of-fit

The specparam model fit, as estimated by MAE and R^2, is illustrated in Fig. 1 for TD children (blue) and children with ASD (red). No specparam model was flagged as underfit (MAE > 0.1, left panel). All potentially overfit models (i.e., a MAE smaller than 0.02) were visually examined ($N = 24$), with the PAF observed to be well modeled in all cases (an example illustrated in the Fig. 1 right panel). As such, no exclusions where made based on MAE. The Fig. 1 middle panel shows the distribution of R^2 values, with an average R^2 of 0.99 (SD = 0.01). The data for the child with an R^2 value of 0.93 were visually examined and determined to be well modeled and thus were retained. Regarding Group differences in model

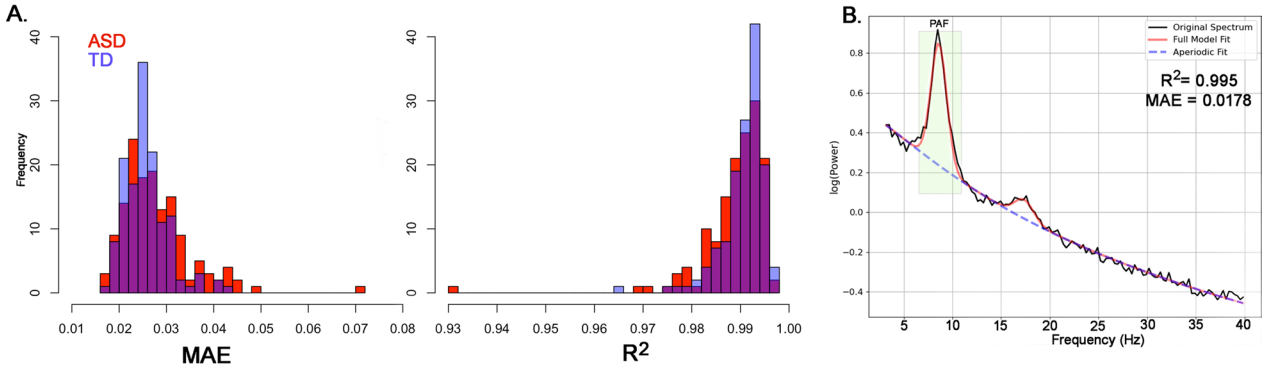

Fig. 1 A: The distribution of MAE values (far left panel) and R^2 values (middle panel). The far-right panel provides an example of the specparam model fit for one participant

goodness-of-fit, at Time 1 TD had better model fits than ASD for R^2 ($p=0.04$) and MAE ($p=0.03$). No Group differences were observed at Time 2 (MAE: $p=0.11$, R^2: $p=0.22$) or Time 3 (MAE: $p=0.30$, R^2: $p=0.18$). As shown in the Online Supplement, the goodness-of-fit values for all children were excellent, with the PAF value correctly identified in children, even those with the lowest goodness-of-fit values.

Maturation of the PAF

The left panel of Fig. 2 shows associations between Age and PAF for both Groups. The LMM predicting PAF with Group and Age as fixed effects and including random intercepts and random slopes, had a slightly lower AIC (AIC = 554) than without random slopes (AIC = 555). As such, the LMM was run with random intercepts and slopes. The LMM results showed PAF increasing with Age by 0.13 Hz/year ($p<0.001$). ASD had a higher PAF than TD by 0.26 Hz ($p=0.02$), thus ASD leading TD by about 2 years. A separate LMM with Group, Age, and the Group x Age interaction showed no interaction effect ($p=0.99$). To further assess Group differences across Time, linear models predicting PAF with Group effects were conducted separately for each Time. Group PAF differences were similar across visits: Time 1 ASD > TD by 0.32 Hz, $p=0.01$, Cohen's $d=0.50$; Time 2 ASD > TD by 0.26 Hz, $p=0.07$, Cohen's $d=0.39$; Time 3 ASD > TD by 0.37 Hz, $p=0.02$, Cohen's $d=0.54$. The right panel of Fig. 2 shows PAF maturation profiles for each child, showing PAF scores rising across Time as expected in most of the children with longitudinal data.

Maturation of optic radiation white-matter

LMMs for each of the four DTI measures were conducted with main effects of Age and Group showing the expected decrease with Age for RD, AD, and MD ($ps<0.001$) and increase with Age for FA ($p<0.01$). No main effect of Group was observed for any of the DTI measures (FA: $p=0.29$; RD: $p=0.67$; MD: $p=0.51$; AD: $p=0.07$). With the Group x Age interaction added to the

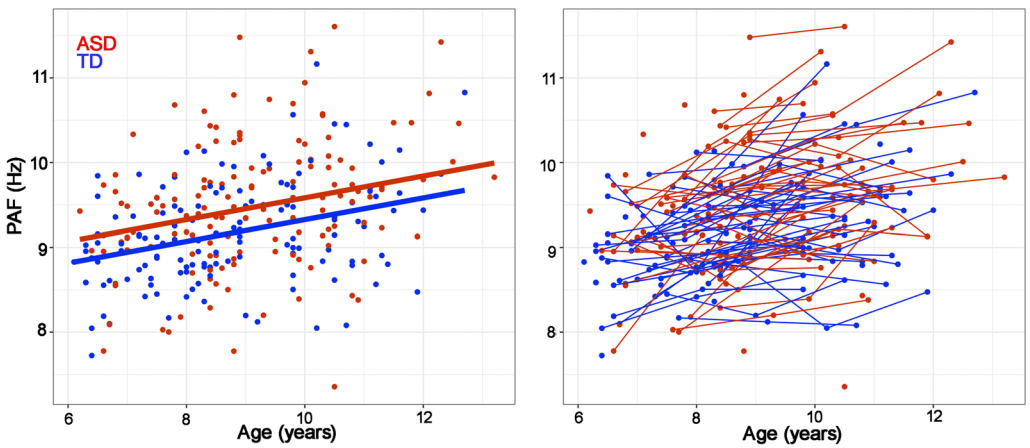

Fig. 2 The left panel shows associations between Age and PAF for TD (blue) and ASD (red). The solid lines show the LMM linear fit line for each Group. The right panel shows PAF maturation profiles for each child across the three visits

model, RD (left panel of Fig. 3) decreased slightly faster for ASD (0.047/year) than TD (0.038/year), a finding that was marginally significant ($p=0.09$). The interaction terms for the FA, AD, and MD did not indicate Group differences ($ps>0.15$). The right panels in Fig. 3 show FA (top row) and RD (bottom row) maturation profiles for each child, showing the expected change in diffusion values across Time in most children.

White matter and PAF associations

Figure 4 shows diffusion and PAF associations for each diffusion measure. LMMs predicting the PAF with DTI and Group as independent variables showed associations between the PAF and all four diffusion measures ($p<0.001$) (Table 2a). When adding the DTI x Group interaction term, a marginally significant interaction between RD and Group was observed ($p=0.08$), with simple-effect analyses suggesting a stronger association between the PAF and RD in ASD than in TD. A LMM for each Group suggested a more negative association between the PAF and RD in ASD ($\beta = -2.07$, $p<0.001$) than TD ($\beta = -0.95$; FA: $p=0.003$). Figure 4 shows the predictions for all four LMMs.

The relationships between the PAF and DTI were further assessed considering Age. As the previous analysis showed a significant correlation between Age and DTI, to remove the collinearity between Age and the DTI measures, Age was residualized by taking the standard residual of linear regression models of Age with each DTI measure. The standard residuals of Age (Age_{resid}) were then included in LMMs, with the PAF the dependent variable, and the DTI measure, Age_{resid}, and Group the independent variables. Table 2b reports beta and p values for each diffusion measure. Negative associations were observed between the PAF and the MD ($p=0.005$), AD ($p=0.046$), and RD ($p=0.001$) measures, and a positive association was observed with FA ($p=0.005$; FA increased by 0.10 and PAF increased by 0.63 Hz). As shown in the final

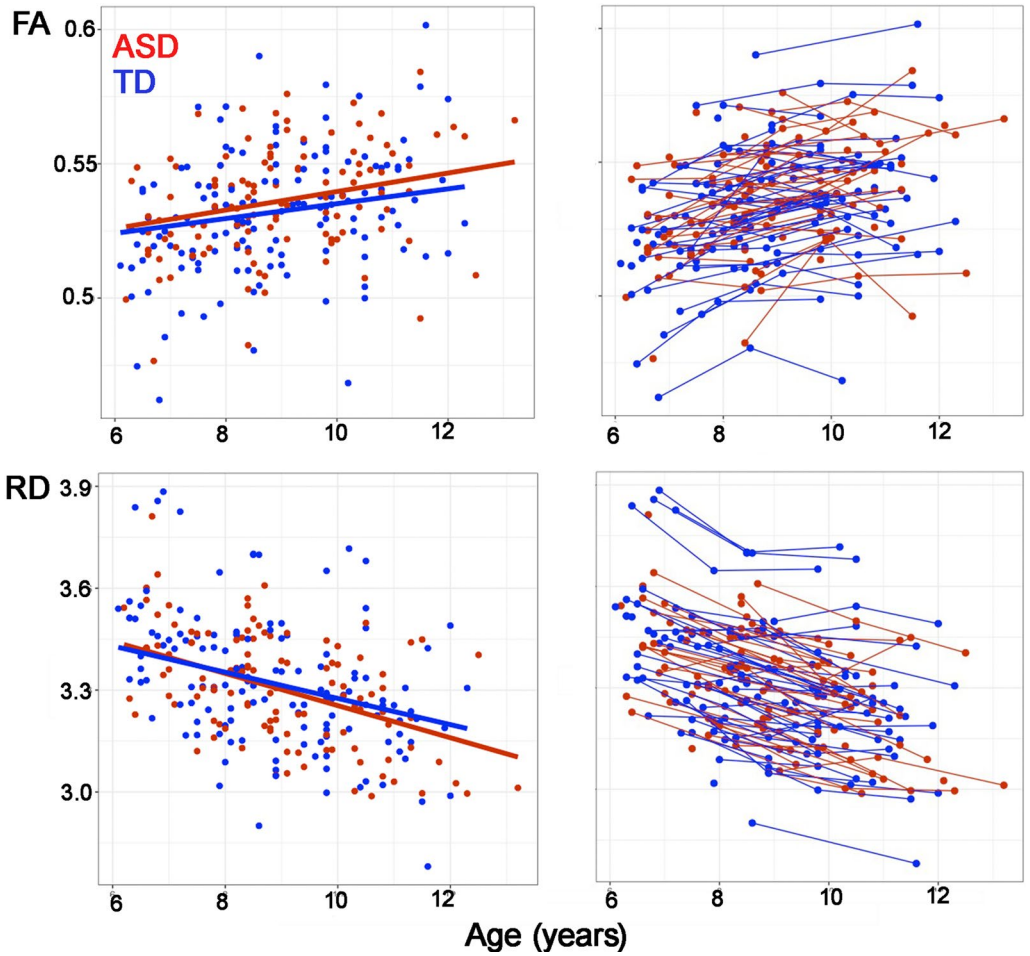

Fig. 3 The left panels show associations between Age and optic radiation diffusion associations for FA (top) and RD (bottom) for TD (blue) and ASD (red). The solid line shows the LMM linear fit line for each Group. The right panels show FA and RD maturation profiles for each child across the three visits

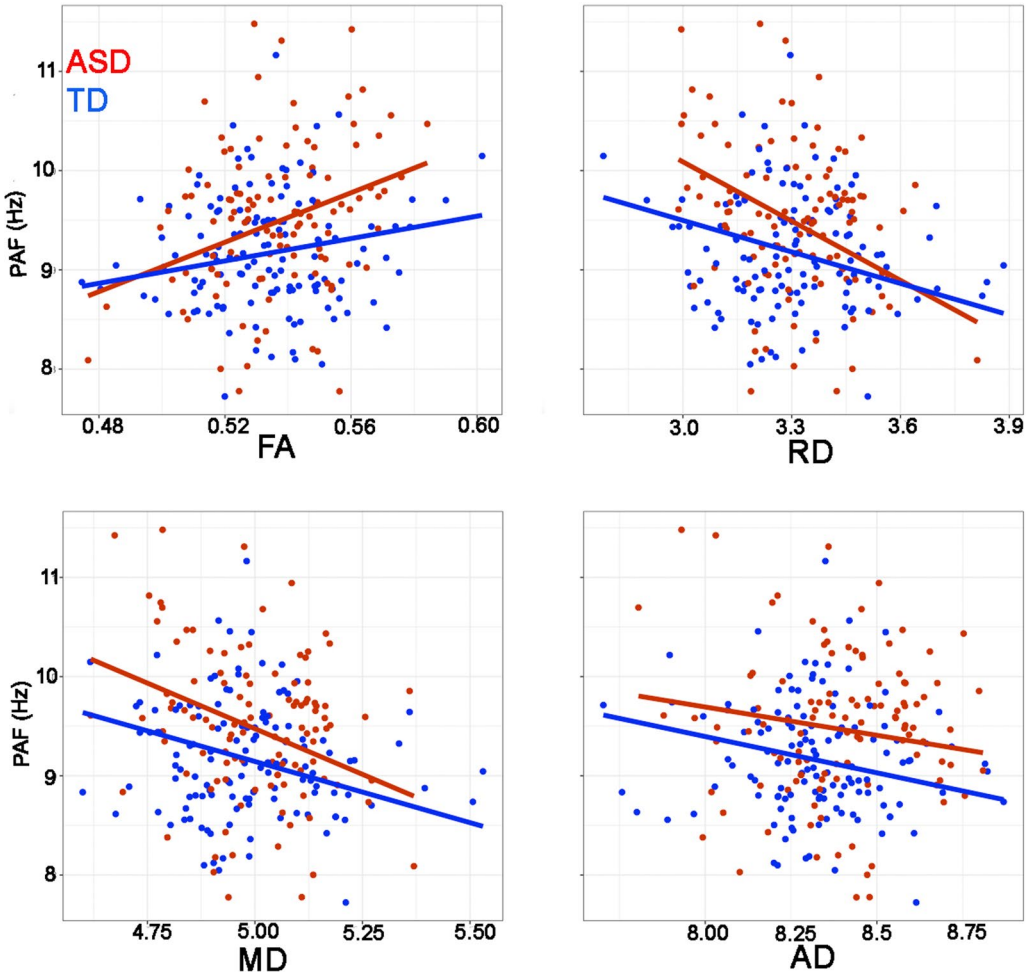

Fig. 4 Association with the PAF for each DTI measure. The red (ASD) and blue (TD) lines show the results of LMMs predicting the PAF with factors: DTI measure, Group, and the DTI x Group interaction

Table 2 With the DTI X Group interaction added, a marginal interaction was observed for RD ($p=0.10$) as well as FA ($p=0.11$)

	a. LMMs ignoring Age		b. LMMs with age residualized		
	DTI	Group	DTI	Age (residualized)	Group
MD	−1.51 ($p<0.001$***)	−0.33 ($p=0.006$**)	−0.96 ($p=0.005$ **)	0.17 ($p<0.001$ ***)	−0.29 ($p=0.01$*)
AD	−0.64 ($p<0.001$***)	−0.35 ($p=0.003$**)	−0.36 ($p=0.046$ *)	0.21 ($p<0.001$ ***)	−0.29 ($p=0.01$*)
RD	−1.48 ($p<0.001$***)	−0.30 ($p=0.01$*)	−0.91 ($p=0.001$ **)	0.17 ($p<0.001$ ***)	−0.29 ($p=0.01$ *)
FA	8.88 ($p<0.001$***)	−0.28 ($p=0.01$*)	6.29 ($p=0.005$ **)	0.19 ($p<0.001$ ***)	−0.28 ($p=0.01$ *)

Separate LMMs for each Group with factors of DTI (RD and FA) and age suggested stronger DTI and PAF associations in ASD (RD: $p<0.01$; FA: $p<0.01$) than TD (RD: $p=0.08$; FA: $p=0.24$)

column of Table 2b, the Group PAF difference remained significant after removing the variance in the PAF associated with white matter.

The PAF and cognitive and symptom associations

Figure 5 shows associations between the PAF and processing speed (left panel), NVIQ (middle panel), and SRS-2 (right panel). A LMM predicting processing speed with the PAF, Group, Age, and a PAF x Group interaction showed a marginally significant interaction ($p=0.06$). Separate LMMs were conducted for each Group, with factors of PAF and Age. As shown in Fig. 5 (left panel), the TD Group showed a main effect of PAF: with a 1 Hz PAF increase, processing speed score increased by 0.86

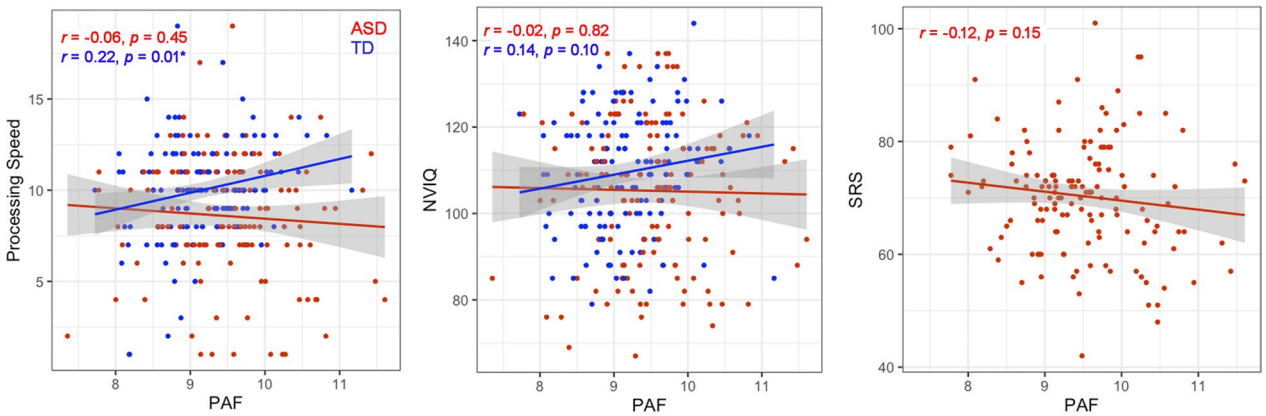

Fig. 5 Scatterplots showing associations between the PAF (x axis) and processing speed (left panel), NVIQ (middle panel) and SRS-2 (right panel) for TD (blue) and ASD (red). Pearson's correlation coefficients (*r*) between cognitive and symptom scores and PAF are shown

points. The ASD Group did not show an association between the PAF and processing speed. As shown in Fig. 5 (middle panel), although the pattern of findings for NVIQ was similar to that observed for processing speed, no main effects or interaction were observed. As shown in Fig. 5 (right panel), no association was observed between the SRS-2 score and the PAF.

Discussion

The present study sought to identify optic radiation white matter as a mechanistic contributor to the TD and ASD differences in the RS PAF. As detailed below, present PAF findings replicate previous studies, with group ASD > TD PAF differences observed at all times (Time 1: 6.1 to 9.3 years old, Time 3: 9.4 to 13.2 years old), and with ASD leading TD by about 2 years. Present findings thus provide additional evidence supporting the use of the RS PAF as a potential brain marker in children with ASD 6 to ~12 years old [26]. The present study also supported the hypothesis of an association between the RS PAF and processing speed in TD but not ASD. The RS PAF and the brain diffusion measures showed expected age-related changes. The brain structure-function findings contribute to the small but growing literature showing that more mature optic radiation white matter supports more efficient transfer of information from the thalamus to the cortex, with more efficient transfer of information associated with a higher PAF. The hypothesis that this brain structure-function association would be absent in the children with ASD was not supported, with white matter predicting the RS PAF in both groups. The following text discusses the present findings with reference to the study hypotheses.

Present longitudinal results extend past cross-sectional findings. The finding of a higher RS PAF in ASD than in TD aligns with cross-sectional studies [22, 28, 32, 73] with a higher PAF in children with ASD than TD observed at all three time points. The finding of higher PAF in young children with ASD compared to TD controls was reported in a subset of this study's Time 1 participants (80% of the current Time 1 sample reported in [73]. The present study showed that group PAF differences are observed until late childhood. The Age x Group interaction reported in Edgar et al. [28], with an age-related maturation of the RS PAF observed in TD but not in ASD (different sample than the present study), was not observed. This is likely due to the age range of the sample; in the present study, the Time 3 subjects were on average 10.8 years old, with previous studies observing TD and ASD maturation differences in children up to 18 years old. Over the next few years, the participants in this study will be followed for an additional three visits (1.5 years between each visit) to further assess the maturation of RS alpha activity in TD and ASD children.

The finding of higher PAF in young children with ASD than in TD suggests that more rapid brain maturation may be occurring in young children with ASD. Findings from other RS studies in ASD support this claim, showing higher PAF in early childhood followed by slower maturation of the RS PAF [22, 28]; and see trending findings in [32, 33]. A review of the literature suggests that this finding of more rapid aspects of brain development early in life is not specific to the RS PAF and extends into structural imaging studies. For instance, more rapid brain development in ASD than in TD in early childhood (from birth to pre-school age) has been reported in structural MRI gray-matter measures [2, 16, 62], connectivity fMRI measures [19, 41], and white-matter measures [6, 8, 31, 70, 75, 89, 91]. In an older cross-sectional sample (5 to 21 years old), DiPiero et al. [24] observed a greater

age-related increase in neurite density in right hemisphere gray matter in ASD compared to the TD group. In general, a growing literature supports the hypothesis put forward at the turn of the 21st century of too rapid early brain development in ASD [17, 18].

In the present study, a higher processing speed score was associated with a higher PAF in TD but not in ASD (the PAF x Group interaction term $p=0.06$), with this finding also observed in a non-overlapping cohort in Edgar et al. [28]. These findings suggest that the differential maturation of the PAF in ASD is related to the loss of an association between brain activity and cognitive ability. The increase in the PAF from infancy to adulthood is thought to reflect the development of large-scale oscillatory networks that facilitate efficient connectivity [68]. This observation is consistent with the proposed role of alpha as a feedback rhythm [87] important for attentional control [45, 47]. The age-related PAF increase likely reflects more efficient neural processing (due in part to maturing thalamocortical white matter – see below), thus resulting in faster neural processing speed. The association between the PAF and processing speed has also been observed in adults, suggesting that this relationship is stable across the lifespan [36, 46]. In the present study, the lack of association between the PAF and processing speed in young children with ASD with average or above-average NVIQ suggests TD and ASD group differences in basic brain encoding processes. As studies including children with below-average NVIQs suggest a positive association between NVIQ and the PAF that is specific to younger children with ASD [32], future work should explore the relationships between the PAF and cognitive ability in children across a broad range of cognitive abilities.

With respect to the optic radiation diffusion measures, group differences in white matter or white-matter maturation were not observed. The ability to detect white-matter group differences may depend on age. For example, Ouyang et al. [64] reported higher FA and lower RD in widespread white-matter tracks in ASD than in TD children before 4 years, and with TD and ASD differences in white-matter maturation resulting in similar white-matter measures by ~4 years of age. The present sample (6 to 12 years old) may capture an age range in which TD and ASD white-matter differences have declined (for detailed discussion of age-dependent brain measures see [27, 28]. Another possibility to be examined in future studies is that group differences in white matter are regionally specific. Studies comparing TD and ASD groups on white-matter maturation throughout the brain and across childhood development are of interest.

Regarding brain structure-function associations, an association between optic radiation white matter (all four DTI measures) and the RS PAF was observed, this finding consistent with the two previous studies [11, 82]. Of note is the similarity between the 0.16 increase in FA associated with a 1 Hz increase in the PAF in the present study and the DTI and FA association reported in Cafarra et al. [11] in children 5 to 21 years old. Our hypothesis of a stronger association between the optic radiation diffusion and the RS PAF in TD than ASD was based on TD and ASD findings showing that in TD children but not children with ASD auditory radiation white matter predicted auditory evoked response latencies [10, 66, 67]. Present findings, however, indicated that in both TD and ASD the maturation of white-matter allows for more efficient thalamo-cortical communication, with faster thalamo-cortical communication resulting in an age-related increase in the RS PAF. Structural brain features other than optic radiation white matter account for variance in the PAF. For example, studies have shown a thalamic contribution [30, 38] as well as a gray-matter cortical thickness contribution [56] to the PAF. It is possible that group differences in these structural measures account for the lost association between the PAF and processing speed in children with ASD.

Several study limitations are of note. Although the sample size is large for a longitudinal multimodal brain imaging study, it is limited in capturing the heterogeneity intrinsic to autism. In a review paper discussing the heterogeneity of autism, Lombardo et al. [53] noted the need for studies that are broad (i.e., large sample size) and deep (i.e., multiple levels of data collected on the same individual). This direction echoes discussions on the reliable detection of brain-behavioral associations, where two paths forward were proposed: (1) large sample studies (i.e., consortium studies) and (2) studies that deeply characterize brain function/anatomy to increase signal-to-noise ratio (SNR) [37]. The present study took steps in this direction by (1) employing multiple levels of data (i.e., behavioral, structural, and functional brain measures) in a longitudinal study design across different age groups, and (2) focusing on the well-studied alpha rhythm, which is a robust measure of neural function with high SNR [29].

In addition to the above heterogeneity concerns, our research addresses two sources of heterogeneity often ignored in pediatric ASD studies. A first source of heterogeneity often ignored in ASD brain-imaging studies is age. As detailed in Edgar [26], given that there are often non-ASD and ASD differences in the rate of brain maturation, pediatric ASD markers will often be age-specific. As such, markers sensitive to ASD differences at one stage of development may be insensitive at another stage. A second source of heterogeneity often ignored in ASD electrophysiology studies is brain location; in particular, a

failure to obtain data that allows assessment of activity at specific brain locations and thus allows for the possibility (and fosters the discovery) of regionally specific group differences as well as to optimally assess brain structure-function associations. The present study addresses these two sources of heterogeneity via examining brain activity within a restricted age range, and via examining the sources of brain activity rather than merely scalp sensor activity (which contains activity from many different brain areas).

Study limitations include a predominantly male sample and the exclusion of children with a NVIQ < 70. Studies including more females are needed to examine sex differences in brain maturation. Additional studies including individuals with below-average NVIQ are needed to evaluate the generalizability of present results. The NVIQ criteria was imposed given the difficulty some individuals with intellectual disability have keeping their eyes closed for an extended time during a RS eyes-closed exam. In a recent study, we showed that an eyes-open dark-room task provides RS alpha measures (alpha power and PAF) comparable to those obtained in the eyes-closed condition [29]. We have found that this task is well-tolerated across the lifespan, with most participants providing several minutes of eyes-open dark-room RS data. We are currently using this task to obtain high signal-to-noise RS measures in infants and children with intellectual disability. Another limitation is that whereas the present study focused on optic radiation white matter, as detailed above, investigating associations between thalamic volume and parietal-occipital gray matter and the PAF are of interest, with the possibility that these (or other) brain measures might account for the group PAF differences. Given the current sample size and the statistical complexity of examining group differences in how multiple brain structure measures are associated with the RS PAF in a longitudinal design (and with missing data), such analyses were beyond the scope of the present study. A final limitation is that the specparam goodness-of-fit measures slightly differed between groups at Time 1. However, the goodness-of-fit measures were very good, the differences between the groups very small (e.g., Time 1 TD $R^2 = 0.987$ and ASD $R^2 = 0.990$), and as shown in the Online Supplement the specparam goodness-of-fit measures were not associated with the ability to detect the PAF.

To conclude, the present longitudinal study replicated prior studies showing a higher PAF in ASD than TD children 6 to 10 years old (ASD leading TD by about 2 years), with the PAF associated with processing speed in TD but not in ASD. Present findings thus provide additional evidence supporting the use of the RS PAF as a functional brain marker in children with ASD 6 to ~12 years old. Both groups showed age-related white matter and RS PAF associations. Overall, the brain structure-function findings contribute to the small but growing literature showing that more mature optic radiation white matter allows for more efficient transfer of information from the thalamus to the cortex, with more efficient transfer of information associated with a higher PAF.

Supplementary Information

The online version contains supplementary material available at https://doi.org/10.1186/s13229-025-00646-4.

Supplementary Material 1

Acknowledgements
The authors gratefully acknowledge the help and support of Yuhan Chen, John Dell, Peter Lam, Rachel Golembski, Na'Keisha Robinson, Erin Verzella, and Shivani Patel.

Author contributions
G.S. and J.C.E. wrote the main manuscript text and prepared figures. H.L.G., R.E.F., M.D., and G.A.M. edited the manuscript. G.S, J.C.E, H.L.G., S.L., and G.A.M conducted the statistical analyses. J.C.E. and J.I.B. developed the research protocol. H.L.G., M.M., R.E.F., M.D., M.K., M.A., S.G., M.K., K.K. E.S.K., L.B., and G.S. participated in data acquisition and analysis. E.S.K., M.K. and L.B. developed the clinical and cognitive assessment battery. H.L.G., M.M., M.D., J.C.E., G.A.M., and G.S. made substantial contributions to the interpretation of the data. All authors substantively contributed. All authors reviewed the manuscript.

Funding
This work was supported by the National Institute of Child Health and Human Development (NICHD) (R01HD093776 to Dr. J. Christopher Edgar) and the National Institute of Mental Health (NIMH) (R01MH107506 to Dr. J. Christopher Edgar; and the National Institute on Deafness and Other Communication Disorders (NIDCD) (K01DC019443) to Dr. Guannan Shen.

Data availability
The data reported in this manuscript are available upon request. Please contact the corresponding author.

Declarations

Competing interests
The authors declare no competing interests.

Human ethics
This study was approved by the Institutional Review Board of Children's Hospital of Philadelphia (IRB 15-012531) and performed in accordance with the Declaration of Helsinki. Parents gave written informed consent and the children gave verbal and written assent.

Author details
[1]Lurie Family Foundations MEG Imaging Center, Department of Radiology, The Children's Hospital of Philadelphia, Philadelphia, PA, USA. [2]Department of Radiology, Perelman School of Medicine, University of Pennsylvania, Philadelphia, PA, USA. [3]Center for Autism Research, Department of Pediatrics, The Children's Hospital of Philadelphia, Philadelphia, PA, USA. [4]Department of Psychiatry, Perelman School of Medicine, University of Pennsylvania, Philadelphia, PA, USA. [5]Department of Psychology, University of Illinois Urbana-Champaign, Urbana-Champaign, IL, USA. [6]Department of Psychology, University of California, Los Angeles, CA, USA. [7]Department of Psychiatry and Biobehavioral Sciences, University of California, Los Angeles, CA, USA. [8]Department of Radiology, Children's Hospital of Philadelphia, Philadelphia, PA 19104, USA.

Received: 16 August 2024 Accepted: 2 February 2025
Published online: 11 March 2025

References

1 Achenbach TM, Rescorla LA. Manual for the ASEBA school-age forms and profiles. In. Burlington: University of Vermont, Research Center for Children, Youth and Families; 2001.
2 Amaral DG, Schumann CM, Nordahl CW. Neuroanatomy of autism. Trends Neurosci. 2008;31(3):137–45. https://doi.org/10.1016/j.tins.2007.12.005.
3 American Psychiatric Association (APA), D.-T. F. Diagnostic and statistical manual of mental disorders: DSM-5 (5th Ed). American Psychiatric Publishing, Inc.; 2013.
4 Andersson JL, Skare S. Distortions in diffusion tensor imaging (DTI): Putting it all together. Vol. 34. In: Proceedings of the international society for magnetic resonance in medicine; 1995. p. 10095.
5 Andersson JLR, Graham MS, Drobnjak I, Zhang H, Filippini N, Bastiani M. Towards a comprehensive framework for movement and distortion correction of diffusion MR images: within volume movement. NeuroImage. 2017;152:450–66. https://doi.org/10.1016/j.neuroimage.2017.02.085.
6 Andrews DS, Lee JK, Solomon M, Rogers SJ, Amaral DG, Nordahl CW. A diffusion-weighted imaging tract-based spatial statistics study of autism spectrum disorder in preschool-aged children. J Neurodev Disord. 2019;11(1):32. https://doi.org/10.1186/s11689-019-9291-z.
7 Angelakis E, Lubar JF, Stathopoulou S, Kounios J. Peak alpha frequency: an electroencephalographic measure of cognitive preparedness. Clin Neurophysiol. 2004;115(4):887–97. https://doi.org/10.1016/j.clinph.2003.11.034.
8 Bashat DB, Kronfeld-Duenias V, Zachor DA, Ekstein PM, Hendler T, Tarrasch R, Sira B, L. Accelerated maturation of white matter in young children with autism: a high b value DWI study. NeuroImage. 2007;37(1):40–7. https://doi.org/10.1016/j.neuroimage.2007.04.060.
9 Bates D, Machler M, Bolker BM, Walker SC. Fitting linear mixed-effects models using lme4. J Stat Softw. 2015;67:1–48.
10 Berman JI, Edgar JC, Blaskey L, Kuschner ES, Levy SE, Ku M, Roberts TP. Multimodal diffusion-MRI and MEG assessment of auditory and language system development in autism spectrum disorder. Front Neuroanat. 2016;10:30. https://doi.org/10.3389/fnana.2016.00030.
11 Caffarra S, Kanopka K, Kruper J, Richie-Halford A, Roy E, Rokem A, Yeatman JD. Development of the alpha rhythm is linked to visual white matter pathways and visual detection performance. J Neurosci. 2024. https://doi.org/10.1523/JNEUROSCI.0684-23.2023.
12 Carter Leno V, Pickles A, van Noordt S, Huberty S, Desjardins J, Webb SJ, Team B. 12-Month peak alpha frequency is a correlate but not a longitudinal predictor of non-verbal cognitive abilities in infants at low and high risk for autism spectrum disorder. Dev Cogn Neurosci. 2021;48:100938. https://doi.org/10.1016/j.dcn.2021.100938.
13 Chiang AK, Rennie CJ, Robinson PA, van Albada SJ, Kerr CC. Age trends and sex differences of alpha rhythms including split alpha peaks. Clin Neurophysiol. 2011;122(8):1505–17. https://doi.org/10.1016/j.clinph.2011.01.040.
14 Constantino JN, Gruber CP. Social responsiveness scale-second edition (SRS-2). Western Psychological Services; 2012.
15 Cornew L, Roberts TP, Blaskey L, Edgar JC. Resting-state oscillatory activity in autism spectrum disorders. J Autism Dev Disord. 2012;42(9):1884–94. https://doi.org/10.1007/s10803-011-1431-6.
16 Courchesne E. Brain development in autism: early overgrowth followed by premature arrest of growth. Ment Retard Dev Disabil Res Rev. 2004;10(2):106–11. https://doi.org/10.1002/mrdd.20020.
17 Courchesne E, Campbell K, Solso S. Brain growth across the life span in autism: age-specific changes in anatomical pathology. Brain Res. 2011;1380:138–45. https://doi.org/10.1016/j.brainres.2010.09.101.
18 Courchesne E, Karns CM, Davis HR, Ziccardi R, Carper RA, Tigue ZD, Courchesne RY. Unusual brain growth patterns in early life in patients with autistic disorder: an MRI study. Neurology. 2001;57(2):245–54.
19 Courchesne E, Pierce K, Schumann CM, Redcay E, Buckwalter JA, Kennedy DP, Morgan J. Mapping early brain development in autism. Neuron. 2007;56(2):399–413. https://doi.org/10.1016/j.neuron.2007.10.016.
20 Cragg L, Kovacevic N, McIntosh AR, Poulsen C, Martinu K, Leonard G, Paus T. Maturation of EEG power spectra in early adolescence: a longitudinal study. Dev Sci. 2011;14(5):935–43. https://doi.org/10.1111/j.1467-7687.2010.01031.x.
21 Di Gregorio F, Trajkovic J, Roperti C, Marcantoni E, Di Luzio P, Avenanti A, Romei V. Tuning alpha rhythms to shape conscious visual perception. Curr Biol. 2022;32(5):988–e998986. https://doi.org/10.1016/j.cub.2022.01.003.
22 Dickinson A, DiStefano C, Senturk D, Jeste SS. Peak alpha frequency is a neural marker of cognitive function across the autism spectrum. Eur J Neurosci. 2018;47(6):643–51. https://doi.org/10.1111/ejn.13645.
23 Dickinson A, Varcin KJ, Sahin M, Nelson CA, Jeste SS. Early patterns of functional brain development associated with autism spectrum disorder in tuberous sclerosis complex. Autism Res. 2019;12(12):1758–73. https://doi.org/10.1002/aur.2193.
24 DiPiero M, Surgent OJ, Travers BG, Alexander AL, Lainhart JE, Iii D, D. C. Gray Matter microstructure differences in autistic males: a gray matter based spatial statistics study. Neuroimage Clin. 2023;37:103306. https://doi.org/10.1016/j.nicl.2022.103306.
25 Donoghue T, Haller M, Peterson EJ, Varma P, Sebastian P, Gao R, Voytek B. Parameterizing neural power spectra into periodic and aperiodic components. Nat Neurosci. 2020;23(12):1655–65. https://doi.org/10.1038/s41593-020-00744-x.
26 Edgar JC. Identifying electrophysiological markers of autism spectrum disorder and schizophrenia against a backdrop of normal brain development. Psychiatry Clin Neurosci. 2020;74(1):1–11. https://doi.org/10.1111/pcn.12927.
27 Edgar JC. Pediatric brain imaging research: brain maturation constrains study design and clinical interpretation. Psychiatry Clin Neurosci. 2021;75(8):267–9. https://doi.org/10.1111/pcn.13278.
28 Edgar JC, Dipiero M, McBride E, Green HL, Berman J, Ku M, Roberts TPL. Abnormal maturation of the resting-state peak alpha frequency in children with autism spectrum disorder. Hum Brain Mapp. 2019. https://doi.org/10.1002/hbm.24598.
29 Edgar JC, Franzen RE, McNamee M, Green HL, Shen G, DiPiero M, Chen Y. A comparison of resting-state eyes-closed and dark-room alpha-band activity in children. Psychophysiology. 2023. https://doi.org/10.1111/psyp.14285.
30 Edgar JC, Heiken K, Chen YH, Herrington JD, Chow V, Liu S, Roberts TP. Resting-state alpha in autism spectrum disorder and alpha associations with thalamic volume. J Autism Dev Disorders. 2015;45(3):795–804. https://doi.org/10.1007/s10803-014-2236-1.
31 Fingher N, Dinstein I, Ben-Shachar M, Haar S, Dale AM, Eyler L, Courchesne E. Toddlers later diagnosed with autism exhibit multiple structural abnormalities in temporal corpus callosum fibers. Cortex. 2017;97:291–305. https://doi.org/10.1016/j.cortex.2016.12.024.
32 Finn CE, Han GT, Naples AJ, Wolf JM, McPartland JC. Development of peak alpha frequency reflects a distinct trajectory of neural maturation in autistic children. Autism Res. 2023;16(11):2077–89. https://doi.org/10.1002/aur.3017.
33 Garcés P, Baumeister S, Mason L, Chatham CH, Holiga S, Dukart J, authorship E-ALg. Resting state EEG power spectrum and functional connectivity in autism: a cross-sectional analysis. Mol Autism. 2022;13(1):22. https://doi.org/10.1186/s13229-022-00500-x.
34 Gioia GA, Isquith PK, Guy SC, Kenworthy L. BRIEF2: behavior rating inventory of executive function. Second Edition. In. Lutz, FL: Psychological Assessment Resources, Inc; 2015.
35 Goldman RI, Stern JM, Engel J, Cohen MS. Simultaneous EEG and fMRI of the alpha rhythm. NeuroReport. 2002;13(18):2487–92. https://doi.org/10.1097/01.wnr.0000047685.08940.d0.
36 Grandy TH, Werkle-Bergner M, Chicherio C, Lövdén M, Schmiedek F, Lindenberger U. Individual alpha peak frequency is related to latent factors of general cognitive abilities. NeuroImage. 2013;79:10–8. https://doi.org/10.1016/j.neuroimage.2013.04.059.
37 Gratton C, Nelson SM, Gordon EM. Brain-behavior correlations: two paths toward reliability. Neuron. 2022;110(9):1446–9. https://doi.org/10.1016/j.neuron.2022.04.018.
38 Green HL, Dipiero M, Koppers S, Berman JI, Bloy L, Liu S, Edgar JC. Peak alpha frequency and thalamic structure in children with typical development and autism spectrum disorder. J Autism Dev Disord. 2022;52(1):103–12. https://doi.org/10.1007/s10803-021-04926-9.

39 Haegens S, Cousijn H, Wallis G, Harrison PJ, Nobre AC. Inter- and intra-individual variability in alpha peak frequency. NeuroImage. 2014a;92(100):46–55. https://doi.org/10.1016/j.neuroimage.2014.01.049.

40 Harms MP, Somerville LH, Ances BM, Andersson J, Barch DM, Bastiani M, Yacoub E. Extending the human Connectome project across ages: imaging protocols for the lifespan development and aging projects. NeuroImage. 2018;183:972–84. https://doi.org/10.1016/j.neuroimage.2018.09.060.

41 He C, Chen H, Uddin LQ, Erramuzpe A, Bonifazi P, Guo X, Duan X. Structure-function connectomics reveals aberrant developmental trajectory occurring at Preadolescence in the autistic brain. Cereb Cortex. 2020;30(9):5028–37. https://doi.org/10.1093/cercor/bhaa098.

42 Hindriks R, Woolrich M, Luckhoo H, Joensson M, Mohseni H, Kringelbach ML, Deco G. Role of white-matter pathways in coordinating alpha oscillations in resting visual cortex. NeuroImage. 2015;106:328–39. https://doi.org/10.1016/j.neuroimage.2014.10.057.

43 Hughes SW, Lőrincz ML, Blethyn K, Kékesi KA, Juhász G, Turmaine M, Crunelli V. Thalamic gap junctions control local neuronal synchrony and influence macroscopic oscillation amplitude during EEG alpha rhythms. Front Psychol. 2011;2:193. https://doi.org/10.3389/fpsyg.2011.00193.

44 Jahnsen H, Llinás R. Electrophysiological properties of guinea-pig thalamic neurones: an in vitro study. J Physiol. 1984;349:205–26. https://doi.org/10.1113/jphysiol.1984.sp015153.

45 Jensen O, Mazaheri A. Shaping functional architecture by oscillatory alpha activity: gating by inhibition. Front Hum Neurosci. 2010;4:186. https://doi.org/10.3389/fnhum.2010.00186.

46 Klimesch W. Memory processes, brain oscillations and EEG synchronization. Int J Psychophysiol. 1996;24(1–2):61–100. https://doi.org/10.1016/s0167-8760(96)00057-8.

47 Klimesch W. Alpha-band oscillations, attention, and controlled access to stored information. Trends Cogn Sci. 2012;16(12):606–17. https://doi.org/10.1016/j.tics.2012.10.007.

48 Klimesch W, Schimke H, Pfurtscheller G. Alpha frequency, cognitive load and memory performance. Brain Topogr. 1993;5(3):241–51. https://doi.org/10.1007/BF01128991.

49 Le Bihan D, Mangin JF, Poupon C, Clark CA, Pappata S, Molko N, Chabriat H. Diffusion tensor imaging: concepts and applications. J Magn Reson Imaging. 2001;13(4):534–46. https://doi.org/10.1002/jmri.1076.

50 Lefebvre A, Delorme R, Delanoë C, Amsellem F, Beggiato A, Germanaud D, Dumas G. Alpha waves as a neuromarker of autism spectrum disorder: the challenge of reproducibility and heterogeneity. Front Neurosci. 2018;12:662. https://doi.org/10.3389/fnins.2018.00662.

51 Levin AR, Naples AJ, Scheffler AW, Webb SJ, Shic F, Sugar CA, entürk D. Day-to-day test-retest reliability of EEG profiles in children with autism spectrum disorder and typical development. Front Integr Neurosci. 2020;14:21. https://doi.org/10.3389/fnint.2020.00021.

52 Liu Z, de Zwart JA, Yao B, van Gelderen P, Kuo LW, Duyn JH. Finding thalamic BOLD correlates to posterior alpha EEG. NeuroImage. 2012;63(3):1060–9. https://doi.org/10.1016/j.neuroimage.2012.08.025.

53 Lombardo MV, Lai MC, Baron-Cohen S. Big data approaches to decomposing heterogeneity across the autism spectrum. Mol Psychiatry. 2019;24(10):1435–50. https://doi.org/10.1038/s41380-018-0321-0.

54 Lopes da Silva FH, Vos JE, Mooibroek J, Van Rotterdam A. Relative contributions of intracortical and thalamo-cortical processes in the generation of alpha rhythms, revealed by partial coherence analysis. Electroencephalogr Clin Neurophysiol. 1980;50(5–6):449–56.

55 Lord C, Rutter M, DiLavore PC, Risi S, Gotham K, Bishop S. Autism Diagnostic Observation Schedule – 2. 2nd Edition. Western Psychological Services; 2012.

56 Mahjoory K, Schoffelen JM, Keitel A, Gross J. The frequency gradient of human resting-state brain oscillations follows cortical hierarchies. Elife. 2020; https://doi.org/10.7554/eLife.53715.

57 Marshall PJ, Bar-Haim Y, Fox NA. Development of the EEG from 5 months to 4 years of age. Clin Neurophysiol. 2002;113(8):1199–208. https://doi.org/10.1016/s1388-2457(02)00163-3.

58 Mathewson KE, Gratton G, Fabiani M, Beck DM, Ro T. To see or not to see: prestimulus alpha phase predicts visual awareness. J Neurosci. 2009;29(9):2725–32. https://doi.org/10.1523/JNEUROSCI.3963-08.2009.

59 Minami S, Oishi H, Takemura H, Amano K. Inter-individual differences in occipital alpha oscillations correlate with white matter tissue properties of the optic radiation. eNeuro. 2020. https://doi.org/10.1523/ENEURO.0224-19.2020.

60 Miskovic V, Ma X, Chou CA, Fan M, Owens M, Sayama H, Gibb BE. Developmental changes in spontaneous electrocortical activity and network organization from early to late childhood. NeuroImage. 2015;118:237–47. https://doi.org/10.1016/j.neuroimage.2015.06.013.

61 Niedermeyer E. (1993). The normal EEG of the waking adult. In N. E, editor, Electroencephalography: basic principles, clinical applications and related fields (4th Edition ed.). Williams and Wilkins.

62 Nordahl CW, Lange N, Li DD, Barnett LA, Lee A, Buonocore MH, Amaral DG. Brain enlargement is associated with regression in preschool-age boys with autism spectrum disorders. Proc Natl Acad Sci U S A. 2011;108(50):20195–200. https://doi.org/10.1073/pnas.1107560108.

63 Ostlund B, Donoghue T, Anaya B, Gunther KE, Karalunas SL, Voytek B, Pérez-Edgar KE. Spectral parameterization for studying neurodevelopment: how and why. Dev Cogn Neurosci. 2022;54:101073. https://doi.org/10.1016/j.dcn.2022.101073.

64 Ouyang M, Cheng H, Mishra V, Gong G, Mosconi MW, Sweeney J, Huang H. Atypical age-dependent effects of autism on white matter microstructure in children of 2–7 years. Hum Brain Mapp. 2016;37(2):819–32. https://doi.org/10.1002/hbm.23073.

65 Richard Clark C, Veltmeyer MD, Hamilton RJ, Simms E, Paul R, Hermens D, Gordon E. Spontaneous alpha peak frequency predicts working memory performance across the age span. Int J Psychophysiol. 2004;53(1):1–9. https://doi.org/10.1016/j.ijpsycho.2003.12.011.

66 Roberts TP, Lanza MR, Dell J, Qasmieh S, Hines K, Blaskey L, Berman JI. Maturational differences in thalamocortical white matter microstructure and auditory evoked response latencies in autism spectrum disorders. Brain Res. 2013;1537:79–85. https://doi.org/10.1016/j.brainres.2013.09.011.

67 Roberts TPL, Bloy L, Ku M, Blaskey L, Jackel CR, Edgar JC, Berman JI. A multimodal study of the contributions of conduction velocity to the auditory evoked neuromagnetic response: anomalies in autism spectrum disorder. Autism Res. 2020;13(10):1730–45. https://doi.org/10.1002/aur.2369.

68 Rodríguez-Martínez EI, Ruiz-Martínez FJ, Paulino B, C. I., Gómez CM. Frequency shift in topography of spontaneous brain rhythms from childhood to adulthood. Cogn Neurodyn. 2017;11(1):23–33. https://doi.org/10.1007/s11571-016-9402-4.

69 Rutter B, Lord. The social communication questionnaire. USA:Western Psychological Services; 2003.

70 Sahyoun CP, Belliveau JW, Mody M. White matter integrity and pictorial reasoning in high-functioning children with autism. Brain Cogn. 2010;73(3):180–8. https://doi.org/10.1016/j.bandc.2010.05.002.

71 Salmelin R, Hari R. Characterization of spontaneous MEG rhythms in healthy adults. Electroencephalogr Clin Neurophysiol. 1994;91:237–48.

72 Samaha J, Postle BR. The speed of Alpha-Band oscillations predicts the temporal resolution of visual perception. Curr Biol. 2015;25(22):2985–90. https://doi.org/10.1016/j.cub.2015.10.007.

73 Shen G, Green HL, Franzen RE, Berman JI, Dipiero M, Mowad TG, Edgar JC. Resting-state activity in children: replicating and extending findings of early maturation of alpha rhythms in Autism Spectrum Disorder. J Autism Dev Disord. 2023. https://doi.org/10.1007/s10803-023-05926-7.

74 Smith SM, Jenkinson M, Woolrich MW, Beckmann CF, Behrens TE, Johansen-Berg H, Matthews PM. Advances in functional and structural MR image analysis and implementation as FSL. Neuroimage, 2004;23(Suppl 1):S208–219. https://doi.org/10.1016/j.neuroimage.2004.07.051.

75 Solso S, Xu R, Proudfoot J, Hagler DJ, Campbell K, Venkatraman V, Courchesne E. Diffusion tensor imaging provides evidence of possible axonal overconnectivity in frontal lobes in autism spectrum disorder toddlers. Biol Psychiatry. 2016;79(8):676–84. https://doi.org/10.1016/j.biopsych.2015.06.029.

76 Somsen RJ, van't Klooster BJ, van der Molen MW, van Leeuwen HM, Licht R. Growth spurts in brain maturation during middle childhood as indexed by EEG power spectra. Biol Psychol. 1997;44(3):187–209.

77 Stephen JM, Hill DE, Candelaria-Cook FT. Examining the effects of prenatal alcohol exposure on corticothalamic connectivity: a multimodal neuroimaging study in children. Dev Cogn Neurosci. 2021;52:101019. https://doi.org/10.1016/j.dcn.2021.101019.

78 Szava S, Valdes P, Biscay R, Galan L, Bosch J, Clark I, Jimenez JC. High resolution quantitative EEG analysis. Brain Topogr. 1994;6(3):211–9.

79 Tournier JD, Mori S, Leemans A. Diffusion tensor imaging and beyond. Magn Reson Med. 2011;65(6):1532–56. https://doi.org/10.1002/mrm.22924.
80 Traub RD, Hawkins K, Adams NE, Hall SP, Simon A, Whittington MA. Layer 4 pyramidal neuron dendritic bursting underlies a post-stimulus visual cortical alpha rhythm. Commun Biol. 2020;3(1):230. https://doi.org/10.1038/s42003-020-0947-8.
81 Tröndle M, Popov T, Dziemian S, Langer N. Decomposing the role of alpha oscillations during brain maturation. Elife. 2022. https://doi.org/10.7554/eLife.77571.
82 Valdes-Hernandez PA, Ojeda-Gonzalez A, Martinez-Montes E, Lage-Castellanos A, Virues-Alba T, Valdes-Urrutia L, Valdes-Sosa PA. White matter architecture rather than cortical surface area correlates with the EEG alpha rhythm. NeuroImage. 2010;49(3):2328–39. https://doi.org/10.1016/j.neuroimage.2009.10.030.
83 Valdés P, Bosch J, Grave R, Hernandez J, Riera J, Pascual R, Biscay R. Frequency domain models of the EEG. Brain Topogr. 1992;4(4):309–19. https://doi.org/10.1007/BF01135568.
84 Van Baal GC, De Geus EJ, Boomsma DI. Genetic architecture of EEG power spectra in early life. Electroencephalogr Clin Neurophysiol. 1996;98(6):502–14.
85 van Beijsterveldt CE, van Baal GC. Twin and family studies of the human electroencephalogram: a review and a meta-analysis. Biol Psychol. 2002;61(1–2):111–38.
86 van Dijk H, Schoffelen JM, Oostenveld R, Jensen O. Prestimulus oscillatory activity in the alpha band predicts visual discrimination ability. J Neurosci. 2008;28(8):1816–23. https://doi.org/10.1523/JNEUROSCI.1853-07.2008.
87 van Kerkoerle T, Self MW, Dagnino B, Gariel-Mathis MA, Poort J, van der Togt C, Roelfsema PR. Alpha and gamma oscillations characterize feedback and feedforward processing in monkey visual cortex. Proc Natl Acad Sci U S A. 2014;111(40):14332–41. https://doi.org/10.1073/pnas.1402773111.
88 Wechsler D. Wechsler intelligence scale for children - (WISC-V): Technical and interpretive manual. 5th ed. ed.). Pearson Clinical Assessment; 2014.
89 Wolff JJ, Gu H, Gerig G, Elison JT, Styner M, Gouttard S, Network I. Differences in white matter fiber tract development present from 6 to 24 months in infants with autism. Am J Psychiatry. 2012;169(6):589–600. https://doi.org/10.1176/appi.ajp.2011.11091447.
90 Woolrich MW, Jbabdi S, Patenaude B, Chappell M, Makni S, Behrens T, Smith SM. Bayesian analysis of neuroimaging data in FSL. NeuroImage. 2009;45(1 Suppl):173–86. https://doi.org/10.1016/j.neuroimage.2008.10.055.
91 Xiao Z, Qiu T, Ke X, Xiao X, Xiao T, Liang F, Liu Y. Autism spectrum disorder as early neurodevelopmental disorder: evidence from the brain imaging abnormalities in 2–3 years old toddlers. J Autism Dev Disord. 2014;44(7):1633–40. https://doi.org/10.1007/s10803-014-2033-x.

Publisher's note